FAILURE OF A CAST-IN-PLACE UNREINFORCED CONCRETE CONDUIT

Jerry C. Chang, Division of Construction and Research,
California Department of Transportation

A case history of the failure of a 72-in. (183-cm) cast-in-place, unreinforced concrete conduit constructed near the toe of a highway embankment is described. Theoretical analysis was conducted to predict the behavior of the conduit. It was concluded that the conduit had failed primarily because of the additional lateral load exerted by a 70-ft-high (21.3-m) embankment. The effectiveness of the theoretical analysis was demonstrated by using actual conduit failure.

•IN September 1969, a 72-in. (183-cm) cast-in-place, unreinforced concrete drainage conduit was placed at the toe of an embankment before the embankment was constructed in the I-10, 57 interchange near San Dimas, Los Angeles County, California (Figure 1). The pipe was constructed by excavating a trench with vertical sides and a semicircular bottom. Forms were then placed in the trench, and the lower half of the pipe was cast first. The forms were then stripped and placed on top of the cast section, and the upper half of the conduit was then poured. The completed conduit has a thickness of 6 in. (15.2 cm). Moderate patching was performed on the interior surface and the exterior surface of the upper half of the conduit. Tests of concrete cylinders indicated an average 28-day compressive strength of 4,490 psi (30 960 kPa).

In October 1969, the trench was backfilled with the previously excavated material and compacted to 90 percent relative compaction. When the backfilling operation was completed, a visual inspection of the conduit revealed no interior cracking or damage.

In April 1970, the highway embankment adjacent to the conduit (Figure 2) was then placed to a height of 20 ft (6.1 m). Another inspection of the conduit indicated no distress. In October through November 1970, the embankment was completed to a height of approximately 70 ft (21.3 m).

In January 1971, a third inspection of the conduit showed extensive cracking, particularly along the spring line of the conduit. The top half of the conduit was laterally displaced away from the embankment by as much as 3 in. (7.6 cm) relative to the bottom half.

Figures 3 and 4 show the crack in the conduit along the spring line and the crown respectively.

SOIL AND FOUNDATION CONDITIONS

When the damage of the conduit was discovered, undisturbed soil samples were taken from boring holes A, B, and C along the conduit (Figure 1). The log of borings showed a moist, silty clay to clayey silt for a depth of approximately 8 ft (2.4 m), a sand layer at 8 to 11 ft (2.4 to 3.4 m), and then silty clay to a depth of 18 ft (5.5 m) (Figure 2). Triaxial compression tests were conducted to determine the shear strength of the soil sample under unsaturated, unconsolidated, and undrained conditions. The test results are given in Table 1.

Publication of this paper sponsored by Committee on Subsurface Structures Design.

Figure 1. Drainage pipe layout.

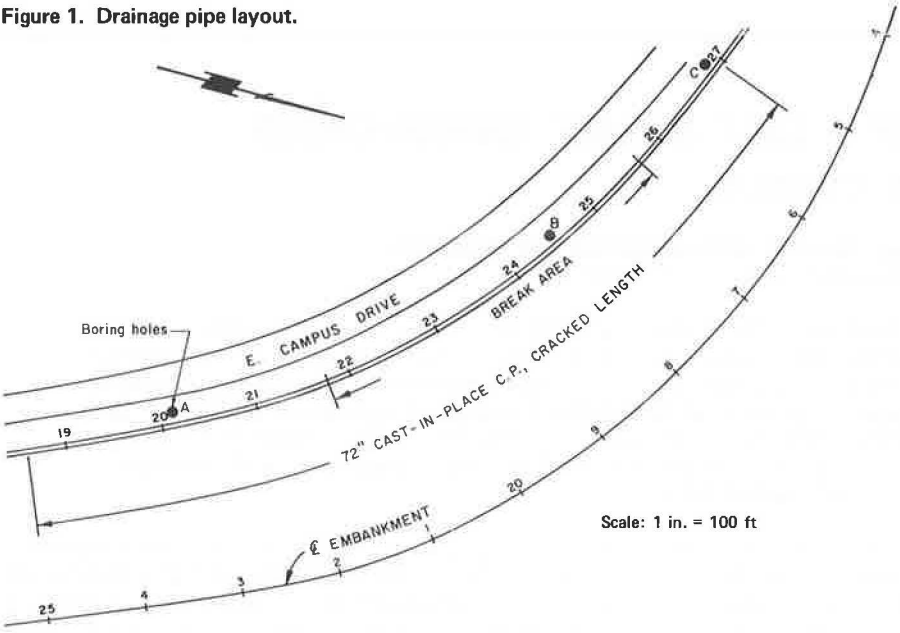

Figure 2. Typical embankment section.

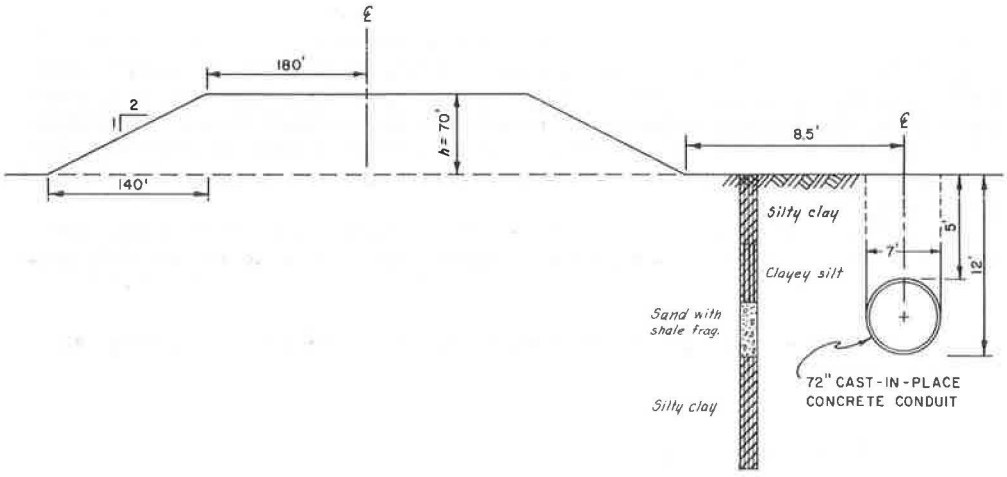

Table 1. Triaxial compression test results.

Depth of Boring (ft)	Soil Type	Wet Unit Weight (lb/ft^3)	Cohesion (lbf/ft^2)	Angle of Internal Friction (deg)
0 to 6	Silty clay	108 to 111	1,200	0
6 to 8	Clayey silt	111 to 124	800	14
8 to 11	Sand with shale fragments	113 to 120	0	34
11 to 18	Silty clay	115 to 118	1,600	10

Note: 1 ft = 0.3 m. 1 lb/ft^3 = 16.02 kg/m^3. 1 lbf/ft^2 = 47.9 Pa.

THEORETICAL ANALYSIS

A theoretical analysis was conducted to determine the stresses developed in the conduit wall because of the local overburden and the load transferred from the highway embankment.

Earth Pressure on Conduit Due to Local Overburden

The vertical earth pressure P_z and the horizontal earth pressure P_x acting on the conduit from the local overburden were computed as follows:

$$P_z = \frac{C_d \gamma B^2}{B} = C_d \gamma B \tag{1}$$

$$P_x = K_o \gamma h \tag{2}$$

where

γ = unit weight of the backfill soil,
B = width of trench,
C_d = load coefficient for ditch conduit,
K_o = coefficient of earth pressure at rest, and
h = height of overburden at section in question.

Equation 1 is based on the equation developed by Spangler for load on a ditch conduit (1). The value of C_d was estimated to be 0.7 from Spangler's chart. Equation 2 is the general equation for estimating earth pressure at rest.

According to Jaky (2),

$$K_o = 1 - \sin\phi \tag{3}$$

where ϕ is the internal friction angle of the soil. Table 2 gives the internal friction angle of the foundation soils. For simplicity in the computation, the K_o value was assumed to be unity in the analysis. The unit weight of soil was estimated to be 135 lb/ft^3 (2160 kg/m^3).

Earth Pressure on Conduit Due to Highway Embankment Load

The earth pressure on the conduit due to the embankment load was estimated for computing subsoil stress at any point A in the foundation soil due to a trapezoidal embankment loading. This pressure was estimated from the equation given by Chang (3), where γ = unit weight of the embankment soil and horizontal stress is

$$\sigma_x = \frac{P}{\pi a}\left[a(\theta_1 + \theta_2 + \theta_3) + B(\theta_1 + \theta_3) + X(\theta_1 - \theta_3) - 2Z\log_e\frac{R_1R_4}{R_2R_3}\right] \tag{4}$$

and vertical subsoil stress is

Figure 3. Cracks in conduit at spring line.

Figure 4. Cracks in conduit at crown.

Figure 5. Subsoil stresses under symmetrical trapezoidal load.

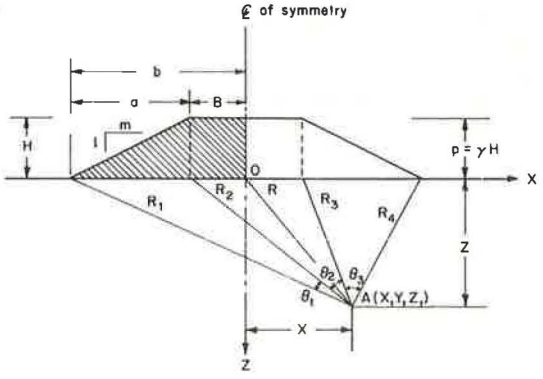

Figure 6. Load of external soil pressure on conduit.

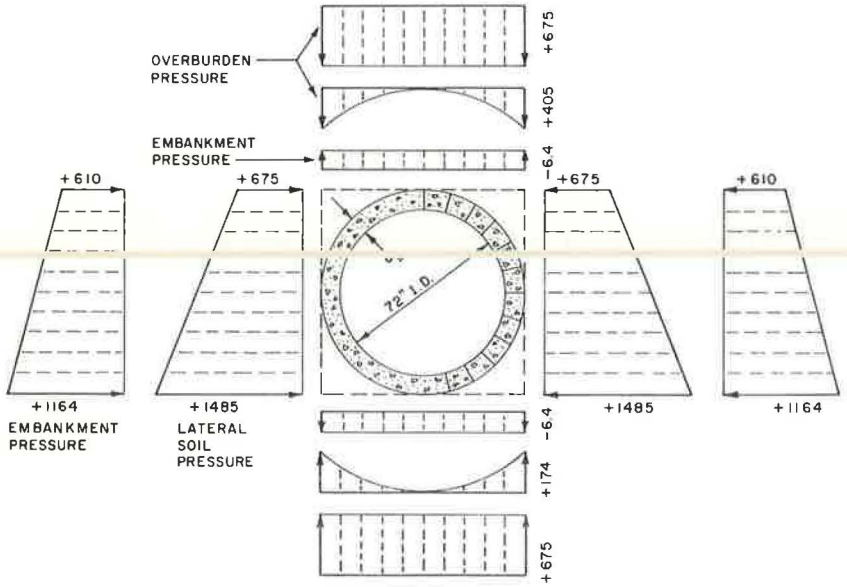

$$\sigma_z = \frac{P}{\pi a}\left[a(\theta_1 + \theta_2 + \theta_3) + B(\theta_1 + \theta_3) + X(\theta_1 - \theta_3)\right] \quad (5)$$

The stresses under a symmetrical trapezoidal load are shown in Figure 5. The loading of the external soil pressure [pounds/foot^2 (pascal)] on the conduit is shown in Figure 6.

Internal Hydrostatic Pressure

When the conduit is flowing full with water, hydrostatic pressure [pounds/foot^2 (pascal)] would act on the internal face of the conduit. The distribution of the water pressure is shown in Figure 7.

Structural Analysis

Structural analysis of the moment, thrust, and shear developed in the conduit wall because of external and internal loads were computed by using the method developed by Phillips and Allen (4). They developed coefficient charts for moment, thrust, and shear for eight shapes of single-barrel conduit by means of Beggs Deformeter apparatus.

The results of moment, thrust, and shear tests are given in Table 2 for external loads and in Table 3 for the combination of external and internal loads. Figures 8, 9, and 10 show the moment, thrust, and shear developed in the conduit wall.

Stress analysis based on the computed result of the moment, thrust, and shear was conducted by using the equation developed by Zanger (5) as follows:

$$\sigma_1 = \frac{1}{2d}\left\{T + \frac{12\ My}{d^2} + \sqrt{\left(T + \frac{12\ My}{d^2}\right)^2 + 9S^2\left[1 - \left(\frac{2y}{d}\right)^2\right]^2}\right\} \quad (6)$$

$$\sigma_2 = \frac{1}{2d}\left\{T + \frac{12\ My}{d^2} - \sqrt{\left(T + \frac{12\ My}{d^2}\right)^2 + 9S^2\left[1 - \left(\frac{2y}{d}\right)^2\right]^2}\right\} \quad (7)$$

$$\tan 2a = 3S\left(\frac{d^2 - 4y^2}{Td^2 + 12\ My}\right) \quad (8)$$

$$\tau_{max} = \frac{1}{2}(\sigma_1 - \sigma_2) \quad (9)$$

where

T = thrust force,
S = shear force,
M = moment,
d = wall thickness of conduit,
x,y = rectangular coordinates,
σ_1, σ_2 = principal stresses,
τ_{max} = maximum shear stress, and
α = angle of orientation of principal stress measured clockwise from x-axis.

Figure 7. Hydrostatic pressure on internal face of conduit.

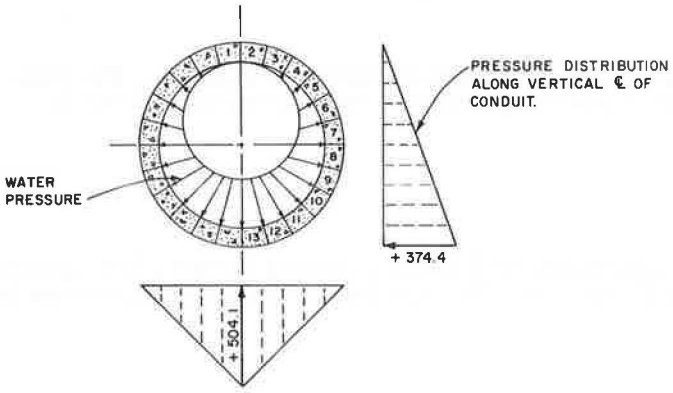

Table 2. Moment, thrust, and shear due to external load.

Section	Moment (lbf-in./in.)	Thrust (lbf-in.)	Shear (lbf-in.)
1	-3,043	+504	0
2	-2,676	+488	-75
3	-1,647	+446	-132
4	-190	+383	-161
5	+1,360	+316	-152
6	+2,612	+261	-101
7	+3,227	+1,385	-20
8	+2,989	+256	+76
9	+1,888	+326	+159
10	+168	+432	+202
11	-1,685	+549	+188
12	-3,103	+639	+112
13	-3,639	+673	0

Note: 1 lbf-in./in. = 4.45 N·m/m. 1 lbf-in. = 0.1130 N-m.

Table 3. Moment, thrust, and shear due to internal and external loads.

Section	Moment (lbf-in./in.)	Thrust (lbf-in.)	Shear (lbf-in.)
1	-2,625	+473	0
4	-94	+361	-143
7	+2,841	+1,375	-13
10	+102	+408	+173
13	-2,990	+610	0

Note: 1 lbf-in./in. = 4.45 N·m/m. 1 lbf-in. = 0.1130 N-m.

Figure 8. Moment in conduit wall.

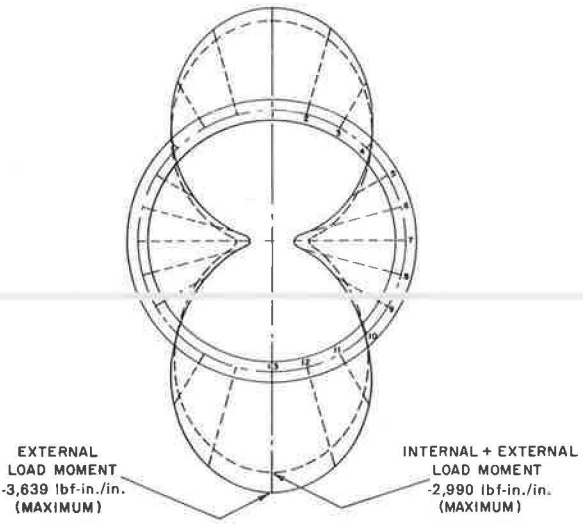

Scale: 1 in. = 3,000 lbf-in./in.

Figure 11 shows the sections cut radially along the wall of the conduit for stress analysis and the relationship among parameters in equations 6, 7, 8, and 9. The analyzed results of principal stresses due to external earth pressure are given in Table 4, and those due to internal water pressure are given in Table 5.

Tensile stresses of more than 400 psi (2760 kPa) developed at the exterior face of the conduit at the top and bottom of the wall (sections 1 and 13), and stresses of more than 300 psi (2070 kPa) developed at the interior face of the wall at the spring line (section 7) (Table 4). A maximum shear stress approaching 400 psi (2760 kPa) developed in the wall at the spring line of the conduit. The computed allowable tensile stress is 217 psi (1496 kPa), and the allowable shear stress is only 113 psi (779 kPa) based on the average 28-day strength of 4,490 psi (30 960 kPa). These stresses are based on the formula given in the 1973 American Concrete Institute Manual of Concrete Practice. Figure 12 shows the locations of the potential cracks in the conduit wall based on the theoretical results of the high tensile stresses.

CONCLUSIONS

Visual inspection, backed by theoretical analysis, indicates that the failure of the conduit was primarily due to the additional lateral load exerted by the 70-ft-high (21.3-m) embankment located about 8.5 ft (2.6 m) away from the conduit. The conduit was cracked first at the inner face along the spring line (also the location of the construction joint). The upper half of the conduit was then sheared off and displaced by as much as 3 in. (7.6 cm) away from the embankment by the lateral earth pressure exerted from the embankment load. Since the lower half of the conduit was cast neatly in the excavated, semicircular-shaped trench, which was mostly composed of sandy soil with shale fragments and was more rigid than the clayey backfill material surrounding the top of the conduit, it was held in place without appreciable movement.

There was no circumferential crack observed on the conduit wall. Therefore, it can be concluded that there was no appreciable uneven settlement along the axis of the conduit. This conduit was replaced with a class 4, double-caged, reinforced concrete pipe after the conclusion of this study in June 1971.

This case history points out the necessity of considering the effects of loads adjacent to the conduit trench as well as those directly over the conduit. The analyzed results have verified the conduit failure and have accurately predicted the locations of cracking of this conduit. I am currently making additional analyses using finite element method and assuming the beam element to be the conduit wall. These results will be reported on in the future.

ACKNOWLEDGMENT

This study was performed for the culvert committee of the California Department of Transportation under the direction of Raymond A. Forsyth. The conduit was constructed under the supervision of Transportation District 07. Particular thanks are extended to District Materials Engineer, J. T. Webster, and Resident Engineer, R. Noad, who provided invaluable information for this paper. Ellsworth L. Chan and Christopher J. Masklee of the Geotechnical Branch, Transportation Laboratory, assisted in the theoretical analysis and preparation of this paper.

REFERENCES

1. M. S. Spangler. Soil Engineering. 1960, pp. 399-401.
2. J. Jaky. Pressure in Silo. Proc., International Conference on Soil Mechanics and Foundation Engineering, Rotterdam, 1948.
3. J. C. Chang. Foundation Stability of Highway Embankments Founded on Deep Clay Soil. Louisiana State Univ., Baton Rouge, Master's thesis, 1964, p. 12.

Figure 9. Thrust in conduit wall.

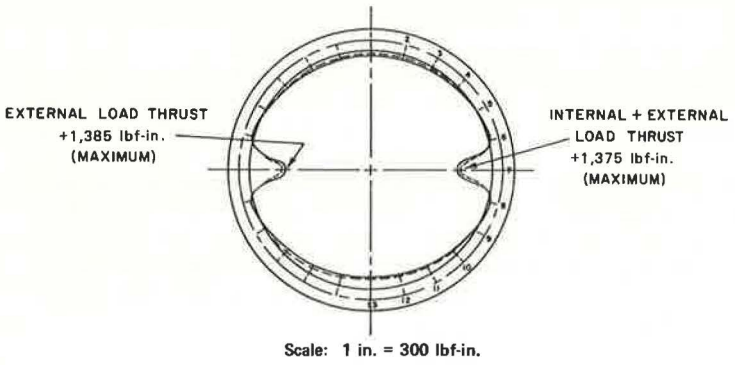

Figure 10. Shear in conduit wall.

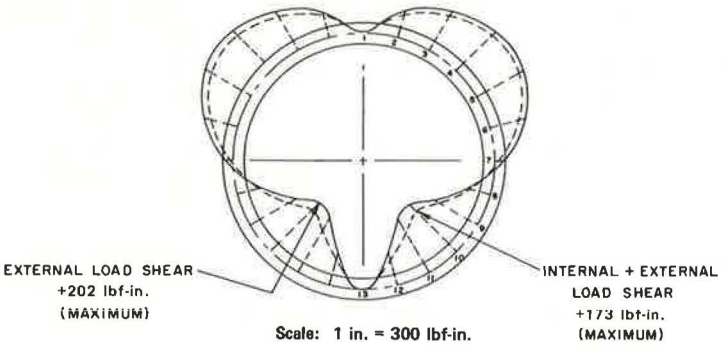

Figure 11. Sections cut radially along conduit wall and relationship among parameters for stress-analysis equations 6, 7, 8, and 9.

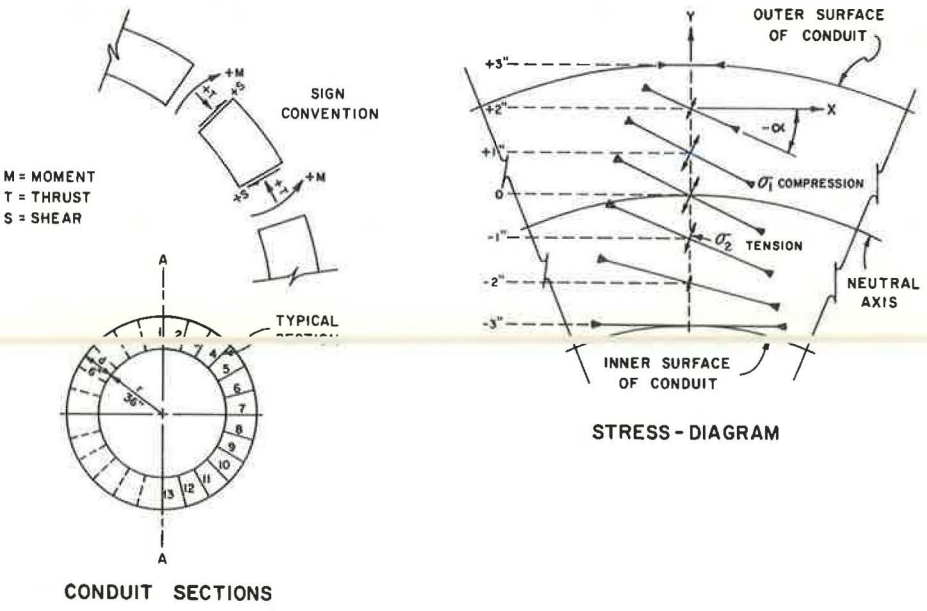

Table 4. Stresses due to external earth pressure.

Section	Y (in.)	σ_1 (psi)	σ_2 (psi)	τ_{max} (psi)	α (deg)
1	+3	0	-423	211	0
	+2	0	-254	127	0
	+1	0	-85	42	0
	0	+84	0	42	0
	-1	+253	0	126	0
	-2	+422	0	211	0
	-3	+591	0	295	0
4	+3	+32	0	16	0
	+2	+52	-9	31	-23
	+1	+71	-18	44	-27
	0	+83	-19	51	-26
	-1	+89	-14	52	-22
	-2	+91	-5	48	-14
	-3	+96	0	48	0
7	+3	+769	0	384	0
	+2	+589	0	295	0
	+1	+410	0	205	-1
	0	+231	0	116	-1
	-1	+52	0	26	-5
	-2	0	-128	64	-1
	-3	0	-307	154	0
10	+3	+100	0	50	0
	+2	+99	-8	53	+16
	+1	+101	-20	61	+27
	0	+98	-26	62	+27
	-1	+86	-23	55	+28
	-2	+65	-12	39	+23
	-3	+44	0	22	0
13	+3	0	-494	247	0
	+2	0	-292	146	0
	+1	0	-90	45	0
	0	+112	0	56	0
	-1	+314	0	157	0
	-2	+517	0	253	0
	-3	+718	0	359	0

Note: Stress sign convention, + = compression, - = tension.
1 in. = 2.5 cm. 1 psi = 6.89 kPa.

Table 5. Stresses due to internal water pressure.

Section	Y (in.)	σ_1 (psi)	σ_2 (psi)	τ_{max} (psi)	α (deg)
1	+3	+65	0	32	0
	+2	+41	0	21	0
	+1	+18	0	9	0
	0	0	-5	3	0
	-1	0	-28	14	0
	-2	0	-52	26	0
	-3	0	-75	37	0
4	+3	+12	0	6	0
	+2	+8	-1	4	+18
	+1	+5	-3	4	+39
	0	+3	-7	4	-34
	-1	+2	-11	6	-21
	-2	0	-15	8	-10
	-3	0	-20	10	0
7	+3	0	-66	33	0
	+2	0	-45	22	-1
	+1	0	-23	12	-4
	0	+1	-3	2	-33
	-1	+20	0	10	+5
	-2	+41	0	21	+1
	-3	+63	0	31	0
10	+3	0	-15	8	0
	+2	+1	-13	7	+18
	+1	+4	-11	8	+30
	0	+6	-10	8	+37
	-1	+6	-7	7	+44
	-2	+6	-3	4	-34
	-3	+7	0	4	0
13	+3	+98	0	49	0
	+2	+62	0	31	0
	+1	+26	0	13	0
	0	0	-11	5	0
	-1	0	-47	23	0
	-2	0	-83	41	0
	-3	0	-119	59	0

Note: Stress sign convention, + = compression, - = tension.
1 in. = 2.5 cm. 1 psi = 6.89 kPa.

Figure 12. Potential crack locations in conduit wall.

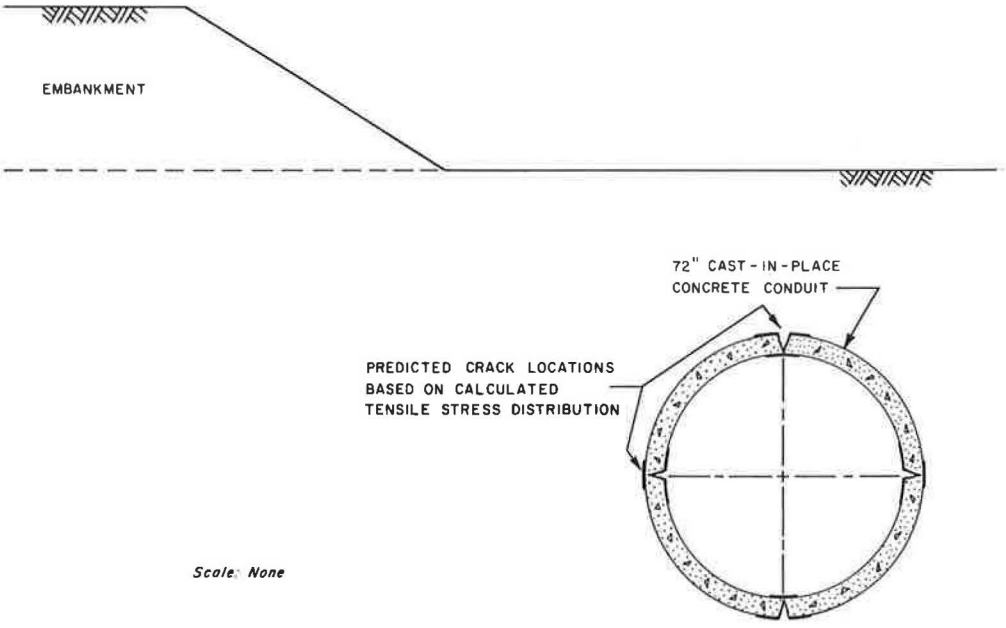

4. H. B. Phillips and I. E. Allen. Beggs Deformeter Stress Analysis of Single-Barrel Conduit. Bureau of Reclamation, U.S. Department of Interior, Denver, 1952.
5. C. N. Zanger. Analytical Determination of Principal Stresses in Structural Members. Bureau of Reclamation, U.S. Department of Interior, Denver, 1948, pp. 2-8.